This is the accepted manuscript made available via CHORUS. The article has been published as:

Twisted rogue-wave pairs in the Sasa-Satsuma equation

Shihua Chen

Phys. Rev. E **88**, 023202 — Published 5 August 2013

DOI: 10.1103/PhysRevE.88.023202

Twisted rogue-wave pairs in the Sasa-Satsuma equation

Shihua Chen

Department of Physics, Southeast University, Nanjing 211189, China

Abstract

Exact explicit rogue wave solutions of the Sasa-Satsuma equation are obtained by use of a Darboux transformation. In addition to the double-peak structure and an analog of the Peregrine soliton, the rogue wave can exhibit an intriguing twisted rogue-wave pair that involves four well-defined zero-amplitude points. This novel structure may enrich our understanding on the nature of rogue waves.

PACS numbers: 47.20.Ky, 42.65.Sf, 42.65.Tg

Keywords: Rogue waves, Sasa-Satsuma equation, Solitons

Sasa-Satsuma equation (SSE), which is so called due to the pioneering work of Sasa and Satsuma [1], is one of a limited number of integrable models and has been a field of active research for the past two decades [1–6]. Thanks to the integrability, the sophisticated soliton construct underlying this wave equation can therefore be achieved using an array of mathematical tools such as inverse scattering transform [1, 2], Riemann problem method [3], Darboux transformation [4], Hirota bilinear method [5], and others. As an extension of the nonlinear Schrödinger (NLS) equation, the SSE contains additional terms explaining the third-order dispersion, the self-steepening, and the self-frequency shift as often found in many important physical applications (e.g., ultrashort pulse propagation in optical fibers [6, 7] and dynamics of deep water waves [8]). In dimensionless form, this equation reads [2, 3]

$$i\psi_t + \frac{\psi_{xx}}{2} + |\psi|^2\psi + i\epsilon[\psi_{xxx} + 3(|\psi|^2)_x\psi + 6|\psi|^2\psi_x] = 0, \tag{1}$$

where $\psi(t, x)$ represents the complex envelope of the wave field, and t and x are the two independent variables. The subscripts stand for the partial derivatives and the real parameter ϵ (> 0) scales the integrable perturbations of the NLS equation. As $\epsilon = 0$, Eq. (1) reduces to the NLS equation which involves only the terms describing the group-velocity dispersion and the self-phase modulation.

With the higher order terms included (although in fixed proportions), Eq. (1) naturally allows for complex intriguing wave dynamics beyond the reach of the NLS equation. Compared to solitons that have been explored over years [1–6], the rational solutions, which are thought of as prototypes of rogue waves [9], are reported only recently. In Ref. [10], Bandelow and Akhmediev pointed out that the lowest-order rogue wave in the SSE can feature a double-peak structure as well as an analog of the Peregrine soliton [11–13], depending on the parameters chosen for the modulationally unstable plane wave. This is distinctly different from that occurred in the Hirota equation where only a tilted Peregrine soliton structure is allowed [14]. However, the rational solution presented in Ref. [10] is overcompacted in form which hinders the broader physics community from understanding the rich dynamics. In this paper, we revisit the fundamental rogue wave in the SSE using a Darboux dressing technique [4] and wish to present an easy-to-catch solution form. More importantly, with the aid of this explicit form, we reveal a novel rogue wave structure—a twisted rogue-wave (TRW) pair, which, to our best knowledge, was never reported before.

As a starting point, we first cast Eq. (1) into a 3×3 linear eigenvalue problem

$$\mathbf{R}_x = \mathbf{U}\mathbf{R}, \qquad \mathbf{R}_t = \mathbf{V}\mathbf{R}, \tag{2}$$

where $\mathbf{R} = (r, s, w)^{\mathcal{T}}$ ($\mathcal{T}$ means a matrix transpose) and

$$\mathbf{U} = \lambda \mathbf{U}_0 + \mathbf{U}_1, \tag{3}$$

$$\mathbf{V} = \lambda^3 \mathbf{V}_0 + \lambda^2 \mathbf{V}_1 + \lambda \mathbf{V}_2 + \mathbf{V}_3, \tag{4}$$

with

$$\mathbf{U}_0 = \frac{1}{6\epsilon} \begin{pmatrix} -2i & 0 & 0 \\ 0 & i & 0 \\ 0 & 0 & i \end{pmatrix}, \tag{5}$$

$$\mathbf{U}_1 = \begin{pmatrix} 0 & -e^{-i\vartheta}\psi & -e^{i\vartheta}\psi^* \\ e^{i\vartheta}\psi^* & 0 & 0 \\ e^{-i\vartheta}\psi & 0 & 0 \end{pmatrix}, \tag{6}$$

$$\mathbf{V}_0 = \frac{1}{4\epsilon}\mathbf{U}_0, \quad \mathbf{V}_1 = \frac{1}{4\epsilon}\mathbf{U}_1, \tag{7}$$

$$\mathbf{V}_2 = -\frac{1}{12\epsilon}\mathbf{U}_0 + \epsilon\left[\mathbf{U}_{1x},\ \mathbf{U}_0\right] + \epsilon \mathbf{U}_1\left[\mathbf{U}_1,\ \mathbf{U}_0\right], \tag{8}$$

$$\mathbf{V}_3 = -\frac{1}{12\epsilon}\mathbf{U}_1 + \epsilon\left[\mathbf{U}_{1x},\ \mathbf{U}_1\right] - \epsilon \mathbf{U}_{1xx} + 2\epsilon \mathbf{U}_1^3. \tag{9}$$

Here $\vartheta = \frac{x}{6\epsilon} - \frac{t}{108\epsilon^2}$, λ is the complex spectral parameter, and $[\ ,\ ]$ denotes the usual matrix commutator. It is easy to show that by virtue of the matrices (3) and (4), Eq. (1) can be exactly reproduced from the compatibility condition $\mathbf{U}_t - \mathbf{V}_x + \mathbf{U}\mathbf{V} - \mathbf{V}\mathbf{U} = 0$. Then, following the standard dressing procedure as in Ref. [4], we can write the resultant Darboux transformation as

$$\psi = \psi_0 + \frac{ie^{i\vartheta}(\lambda - \lambda^*)}{2\epsilon} \frac{(\alpha r + \beta r^*)s^* + (\alpha r^* + \beta^* r)w}{\alpha^2 - |\beta|^2}, \tag{10}$$

with

$$\alpha = |r|^2 + |s|^2 + |w|^2, \tag{11}$$

$$\beta = \frac{\lambda^* - \lambda}{2\lambda}\left(r^2 + 2sw\right), \tag{12}$$

where ψ_0 and ψ denote the seeding and the new solutions of Eq. (1), respectively, and r, s and w are λ-dependent functions determined by the seeding solution ψ_0.

As is well known, the rogue wave solutions represent the limiting case of either Ma solitons [15] or Akhmediev breathers [16], and are tightly related to the modulationally unstable plane waves [4, 9, 10, 12]. Hence, we start directly with the plane-wave solution

$$\psi_0(t,x) = \frac{c}{2\epsilon}\exp\left[-\frac{i}{2\epsilon}\left(kx - \frac{\omega}{4\epsilon}t\right)\right], \tag{13}$$

where $c > 0$ and the dispersion relation reads

$$\omega = 2c^2(1+3k) - k^2 - k^3. \tag{14}$$

Substitution of Eq. (13) into Eq. (2) followed by some algebraic simplification yields

$$r(\lambda) = e^{i\theta_1} + \Gamma_1 e^{i\theta_2} + \Gamma_2 e^{i\theta_3}, \tag{15}$$

$$s(\lambda) = \frac{2\epsilon}{c} e^{i\vartheta} f_1 \psi_0^* r(\lambda), \tag{16}$$

$$w(\lambda) = \frac{2\epsilon}{c} e^{-i\vartheta} f_2 \psi_0 r(\lambda), \tag{17}$$

where Γ_1 and Γ_2 are arbitrary constants, and

$$\theta_j = \frac{\mu_j}{6\epsilon}x - \frac{\nu_j}{216\epsilon^2}t, \tag{18}$$

$$\begin{aligned}\nu_j = {} & 3\lambda\mu_j^2 + (3 + 36c^2 - K^2 - 6\lambda^2)\mu_j \\ & -6\lambda^3 - 2\lambda(18c^2 + K^2),\end{aligned} \tag{19}$$

$$f_1 = \frac{r_{11}e^{i\theta_1} + \Gamma_1 r_{12} e^{i\theta_2} + \Gamma_2 r_{13} e^{i\theta_3}}{e^{i\theta_1} + \Gamma_1 e^{i\theta_2} + \Gamma_2 e^{i\theta_3}}, \tag{20}$$

$$f_2 = \frac{r_{21}e^{i\theta_1} + \Gamma_1 r_{22} e^{i\theta_2} + \Gamma_2 r_{23} e^{i\theta_3}}{e^{i\theta_1} + \Gamma_1 e^{i\theta_2} + \Gamma_2 e^{i\theta_3}}, \tag{21}$$

with

$$r_{1j} = -\frac{3ic}{\mu_j - \lambda + K}, \quad r_{2j} = -\frac{3ic}{\mu_j - \lambda - K}. \tag{22}$$

Here $K \equiv 1 + 3k$, the index j runs over 1, 2, and 3, and μ_j are three roots of the cubic equation

$$\mu^3 - \left(3\lambda^2 + 18c^2 + K^2\right)\mu + 2\lambda\left(\lambda^2 + 9c^2 - K^2\right) = 0. \tag{23}$$

At this stage, by substituting Eqs. (15)–(17) into the Darboux transformation (10), one can readily obtain the general breather solutions of Eq. (1) termed Ma solitons or Akhmediev breathers, depending on the choice of the arbitrary complex parameter λ. Interestingly, a special choice of the value of λ such that Eq. (23) has two equal roots can reduce these two kinds of breather solutions, which always take an otherwise exponential form, into the same rational solutions termed rogue waves. For that purpose, we inspect the cubic equation (23) and find that as

$$\lambda = \frac{\kappa}{6}\left(3 - \frac{\kappa^2+\eta^2}{K^2}\right) \pm \frac{i\eta}{6}\left(3 + \frac{\kappa^2+\eta^2}{K^2}\right) \equiv \lambda', \tag{24}$$

where

$$\kappa = \frac{\sqrt{2}}{2}\left[\sqrt{K^2(18c^2+K^2)} - 9c^2 + K^2\right]^{1/2}, \tag{25}$$

$$\eta = \frac{\sqrt{2}}{2}\left[\sqrt{K^2(18c^2+K^2)} + 9c^2 - K^2\right]^{1/2}, \tag{26}$$

it will allow a special set of roots

$$\mu_1 = \mu_2 = -\mu_3/2 = \mu', \tag{27}$$

with

$$\mu' = -\frac{\kappa\eta^2}{27c^2}\left(1 + \frac{\kappa^2+\eta^2}{K^2}\right) \pm \frac{i\kappa^2\eta}{27c^2}\left(1 - \frac{\kappa^2+\eta^2}{K^2}\right). \tag{28}$$

It is noteworthy that we have exactly separated the complex parameter λ', and hence μ', into the real and imaginary parts. Obviously, in order for κ and η to be real, the parametric condition $4K^2 \geqslant 9c^2$ should hold, which defines the allowed regime of k. Under the circumstances, by setting $\Gamma_1 = -1$ and $\Gamma_2 = 0$ in Eqs. (20) and (21), f_1 and f_2 will take the simple rational forms

$$f_1(\lambda') = -\frac{3ic}{\mu' - \lambda' + K} - \frac{36\epsilon^2(2\mu' + \lambda' - K)}{cK\chi}, \tag{29}$$

$$f_2(\lambda') = -\frac{3ic}{\mu' - \lambda' - K} + \frac{36\epsilon^2(2\mu' + \lambda' + K)}{cK\chi}, \tag{30}$$

where χ is a linear function of t and x, given by

$$\chi = (6\lambda'\mu' - 6\lambda'^2 + 3 + 36c^2 - K^2)t - 36\epsilon x. \tag{31}$$

Consequently, we insert Eqs. (15)–(17) into Eq. (10) for this specific value λ' and, with tedious manipulations, we obtain the exact fundamental rogue wave solution

$$\psi(t,x) = \psi_0(t,x)\left(1 - \frac{G+iH}{D}\right), \tag{32}$$

where

$$\begin{aligned} G = {} & \frac{\epsilon^2(9c^2+2K^2)}{2c^2K^2}\left(\xi + \frac{4\kappa^2\eta^2}{9c^2+2K^2}t\right)^2 \\ & + \frac{8\epsilon^2\kappa^2\eta^2(\kappa^2-\eta^2)}{c^2(9c^2+2K^2)}t^2 + \frac{162\epsilon^6(9c^2+2K^2)^3}{c^2\kappa^2\eta^2(\kappa^2+\eta^2)^2}, \end{aligned} \tag{33}$$

$$H = \frac{1}{2K}\left[\frac{\xi^2}{4} + \kappa^2\eta^2 t^2 - \frac{243\epsilon^4(9c^2+2K^2)^2}{\kappa^2\eta^2(18c^2+K^2)}\right] \times \left(\xi + \frac{4\kappa^2\eta^2}{9c^2}t\right) + \frac{16\epsilon^4\kappa^2\eta^2(27c^2+2K^2)}{c^4K(18c^2+K^2)}t, \tag{34}$$

$$D = \frac{1}{36\epsilon^2}\left[\frac{\xi^2}{4} + \kappa^2\eta^2 t^2 + \frac{18^2\epsilon^4(\kappa^4-\kappa^2\eta^2-\eta^4)}{\kappa^2\eta^2(\kappa^2+\eta^2)}\right]^2 + \frac{9\epsilon^2\eta^2}{(\kappa^2+\eta^2)^2}\left(\xi+2\kappa^2 t\right)^2 + \frac{108^2\epsilon^6}{\eta^2(\kappa^2+\eta^2)}, \tag{35}$$

with

$$\xi = (K^2 - 1 - 27c^2)t + 12\epsilon x. \tag{36}$$

Noting here that we have translated the solution along both t and x in order to make its central value close to the origin [17], and simplified it to the most explicit form by expressing G, H and D as real polynomials of t and x. We highlight that this general rational solution is one of the central results we wish to present here, and as will be shown, it can give a clear picture of the full dynamics of the fundamental rogue waves governed by the SSE. Furthermore, owing to the fourth-order polynomial being involved in D, we expect there to be a significantly more complicated structure than does the Peregrine soliton which only involves polynomials of second order [9, 11–14]. For distinctness, we will term this solution the SSE rogue wave.

Indeed, as $\epsilon = 0$ and for a general plane-wave seed $\psi_0(t,x) = ae^{-i[bx+(b^2/2-a^2)t]}$ (a and b are real constants) which corresponds to Eq. (13) with $c = 2a\epsilon$ and $k = 2b\epsilon$, our rogue wave solution (32) can be readily reduced to

$$\psi(t,x) = \psi_0(t,x)\left[1 - \frac{4(2ia^2t+1)}{1+4a^2(x+bt)^2+4a^4t^2}\right], \tag{37}$$

which is exactly the Peregrine soliton solution of the standard NLS equation [11–13]. This fact suggests that the Peregrine soliton, while keeping its peak amplitude always three times the background height, is only the simple limiting case of the SSE rogue wave.

Further inspection of Eq. (32) shows that the SSE rogue wave has a central amplitude

$$|\psi(0,0)| = 3|\psi_0|\left|\frac{9c^2-2K^2}{9c^2+2K^2}\right|, \tag{38}$$

which evolves from $|\psi_0|$ at $|K| = 3c/2$ to zero at $|K| = 3c/\sqrt{2}$, and then to $3|\psi_0|$ as $|K| = \infty$, see the blue lines in Fig. 1. It is clear from the foregoing discussions that as $|K| < 3c/2$,

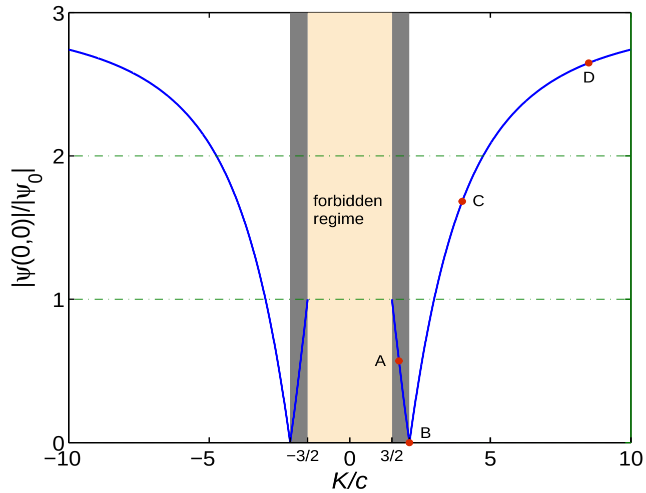

FIG. 1. (Color online) Central amplitude of the SSE rogue wave (normalized to $|\psi_0|$) versus K (normalized to c) in the allowed regime $|K| \geqslant 3c/2$. Points A, B, C and D indicate the central amplitudes for $k = 0.25$, 0.3738, 1 and 2.5, respectively.

corresponding to the pink region in Fig. 1, no rogue waves are allowed. This is exactly consistent with the parametric condition obtained from the linear stability analysis, see Refs. [4, 10]. Moreover, for such a rogue wave, there always exist two characteristic points (t_0, x_0)

$$t_0 = \pm\left[\frac{81\epsilon^4(9c^2+2K^2)^2(27^2c^4-99c^2K^2-4K^4)}{2\kappa^4\eta^4(\kappa^2+\eta^2)^2(27c^2+4K^2)} + \frac{18\epsilon^4\sqrt{81c^2+2K^2}(9c^2+2K^2)^{3/2}}{c^2\kappa^2\eta^2(\kappa^2+\eta^2)(27c^2+4K^2)}\right]^{1/2}, \tag{39}$$

$$x_0 = \frac{1701c^4+27c^2-225c^2K^2-8K^4}{18^2\epsilon c^2}t_0 - \frac{2\kappa^4\eta^4(\kappa^2+\eta^2)^2(27c^2+4K^2)}{162^2\epsilon^5c^2(9c^2+2K^2)^2}t_0^3, \tag{40}$$

that fulfill $H = 0$ and $D - G = 0$, or equivalently, $|\psi(t_0, x_0)| = 0$. For this reason, we term such two characteristic points the zero-amplitude points, namely, the wave amplitude falls to zero at these points [17]. Evidently, as $\epsilon = 0$, Eqs. (39) and (40) can boil down to the two zero-amplitude points $(0, \pm\sqrt{3}/2a)$ of the Peregrine soliton (37) which locate symmetrically on the x axis.

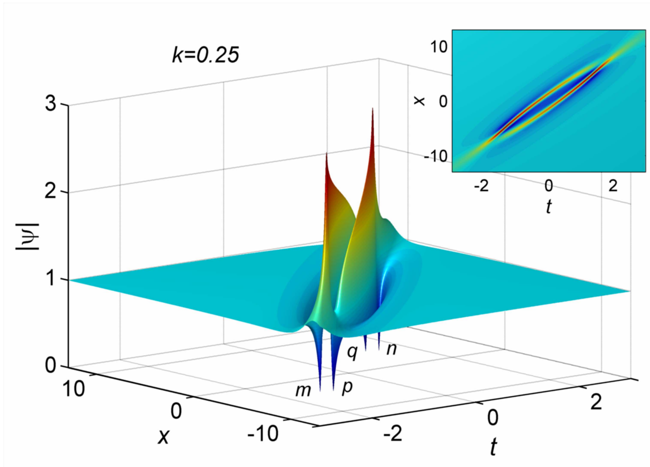

FIG. 2. (Color online) TRW pair defined with four zero-amplitude points m, n, p and q for $k = 0.25$ and $c = 2\epsilon = 1$. The inset shows the corresponding contour distribution.

More interestingly, as $3c/2 < |K| < 3c/\sqrt{2}$, corresponding to the grey regions in Fig. 1, there will appear additional two zero-amplitude points which can also be represented by the formulas (39) and (40) if only replacing the "+" sign between two terms in Eq. (39) (inside square brackets) by the "−" one. These two newly emerging points, along with the two given by Eqs. (39) and (40), can define a TRW pair. We demonstrate this intriguing structure in Fig. 2 by using a typical value $k = 0.25$ and letting $c = 2\epsilon = 1$, for which the central amplitude is denoted by the point A in Fig. 1. Meanwhile, we have indicated the four zero-amplitude points by m, n, p and q, whose coordinates read as $(-1.3888, -4.3976)$, $(1.3888, 4.3976)$, $(-1.1802, -4.6499)$ and $(1.1802, 4.6499)$, respectively. It is shown that this TRW pair consists of two extended rogue-wave components which curve towards each other and have an identical but antisymmetric shape (see inset). Further, we find that as $|K| \to 3c/2$, this rogue wave pair will become infinitely extended and will evolve towards a two-soliton state on a nonzero background. However, as $|K| = 3c/\sqrt{2}$, the TRW pair reduces to the rogue wave that has three zero-amplitude points, as seen in Figs. 3(a) and 3(b). For this special case, the zero-amplitude points p and q in Fig. 2 merge completely and become one at the center, while the two outer points m and n remain.

Once $|K| > 3c/\sqrt{2}$, the TRW pair is unable to survive as the zero-amplitude points p and q disappear entirely. In this case, the SSE rogue wave generally exhibits much less complicated structure. This can be seen in Fig. 3 where the SSE rogue wave will evolve into

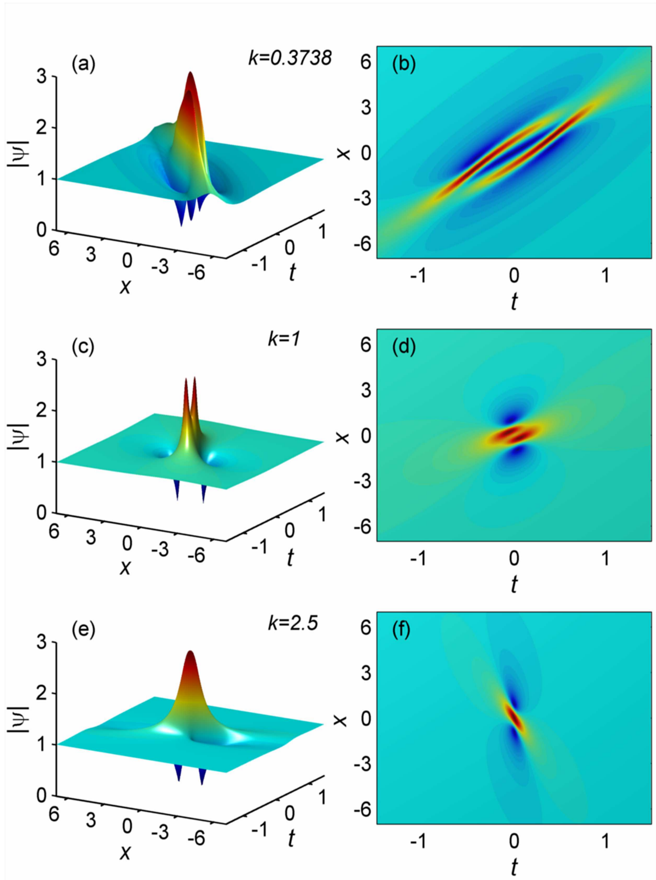

FIG. 3. (Color online) Characteristic structures of the SSE rogue wave as $|K| \geqslant 3c/\sqrt{2}$. (a), (c) and (e) display the rogue wave structure with three zero-amplitude points, the double-peak structure, and the usual Peregrine-soliton-like structure, respectively, each obtained with $k = 0.3738$, 1 and 2.5 accordingly. (b), (d) and (f) in the right column show the corresponding contour distributions. Other parameters are the same as in Fig. 2.

a double-peak structure for $k = 1$ [see Figs. 3(c) and 3(d)] and an analog of the Peregrine soliton for $k = 2.5$ [see Figs. 3(e) and 3(f)], as have been demonstrated in Ref. [10]. Both types of structures involve only two zero-amplitude points as specified by Eqs. (39) and (40), and have central amplitudes always smaller than three times the background height, as indicated by the points C and D in Fig. 1. A direct comparison between Figs. 3(b), 3(d) and 3(f) shows that as $|K|$ grows, the SSE rogue wave, apart from having a simpler structure, will be significantly reduced in t dimension. Particularly, as $|K| \to \infty$, the zero-amplitude points approach invariably towards $(0, \pm\sqrt{3}\epsilon/c)$ and the SSE rogue wave will take the simple form of the line rogue wave [18].

Finally, let us give some remarks on the stability of the SSE rogue wave. Unsurprisingly, as a unique wave event, though it would appear unexpectedly [9], each of the rogue wave structures should be stable. We notice that the Peregrine soliton, which is the limiting case of our SSE rogue wave, can exhibit robustness against perturbations [19] and has been observed in a water wave tank [12] and in optical fibers [13]. Significantly, in recent work Ankiewicz *et al.* have partially lifted the restriction on the parameters of the SSE and found similar rogue wave structures as in unperturbed case [20]. This is no doubt an evidence of the stability of the SSE rogue wave and thus offers the possibility to realize its rich structure experimentally [7].

In summary, we presented the most explicit rogue wave solutions of the SSE by use of a Darboux transformation. We demonstrated that, in addition to the double-peak structure and a Peregrine-soliton-like structure as exhibited in Ref. [10], the SSE rogue wave can feature an intriguing TRW pair that only survives for $3c/2 < |K| < 3c/\sqrt{2}$. We also provided exact explicit formulas for defining the four zero-amplitude points peculiar to the TRW structure as well as the central amplitude involved, of course including those for other rogue wave structures. We anticipate that this well-defined TRW structure may also contribute to the existing signatures of rogue waves [9].

This work was partially supported by the Qing Lan Project, the National Natural Science Foundation of China (Grant No. 11174050), the Natural Science Foundation of Jiangsu Province of China (Grant No. BK2011586), and the Scientific Research Foundation for the Returned Overseas Chinese Scholars, SEM.

[1] N. Sasa and J. Satsuma, J. Phys. Soc. Jpn. **60**, 409 (1991).

[2] D. Mihalache, L. Torner, F. Moldoveanu, N.-C. Panoiu, and N. Truta, J. Phys. A: Math. Gen. **26**, L757 (1993).

[3] D. Mihalache, N.-C. Panoiu, F. Moldoveanu, and D.-M. Baboiu, J. Phys. A: Math. Gen. **27**, 6177 (1994).

[4] O. C. Wright III, Chaos Solitons and Fractals **33**, 374 (2007).

[5] C. Gilson, J. Hietarinta, J. Nimmo, and Y. Ohta, Phys. Rev. E **68**, 016614 (2003).

[6] D. Mihalache, N. Truta, and L.-C. Crasovan, Phys. Rev. E **56**, 1064 (1997).

[7] D. R. Solli, C. Ropers, P. Koonath, and B. Jalali, Nature **450**, 1054 (2007).

[8] A.V. Slunyaev, J. Exp. Theor. Phys. **101**, 926 (2005); A. R. Osborne, *Nonlinear Ocean Waves and the Inverse Scattering Transform* (Academic, San Diego, 2010).

[9] N. Akhmediev, A. Ankiewicz, and M. Taki, Phys. Lett. A **373,** 675 (2009); N. Akhmediev, J. M. Soto-Crespo, and A. Ankiewicz, Phys. Lett. A **373,** 2137 (2009).

[10] U. Bandelow and N. Akhmediev, Phys. Rev. E **86**, 026606 (2012); U. Bandelowa and N. Akhmediev, Phys. Lett. A **376**, 1158 (2012).

[11] D. H. Peregrine, J. Aust. Math. Soc. Series B, Appl. Math. **25**, 16 (1983).

[12] A. Chabchoub, N. P. Hoffmann, and N. Akhmediev, Phys. Rev. Lett. **106,** 204502 (2011).

[13] B. Kibler, J. Fatome, C. Finot, G. Millot, F. Dias, G. Genty, N. Akhmediev, and J. M. Dudley, Nature Phys. **6,** 790 (2010).

[14] A. Ankiewicz, J. M. Soto-Crespo, and N. Akhmediev, Phys. Rev. E **81**, 046602 (2010).

[15] Y. C. Ma, Stud. Appl. Math. **60**, 43 (1979).

[16] N. Akhmediev and V. I. Korneev, Theor. Math. Phys. **69**, 1089 (1986).

[17] S. Chen and L.-Y. Song, Rev. Rev. E **87**, 032910 (2013).

[18] Y. Ohta and J. Yang, Rev. Rev. E **86**, 036604 (2012).

[19] A. Ankiewicz, N. Devine, and N. Akhmediev, Phys. Lett. A **373**, 3997 (2009).

[20] A. Ankiewicz, J. M. Soto-Crespo, M. A. Chowdhury, and N. Akhmediev, J. Opt. Soc. Am. B **30**, 87 (2013).